GEOPHYSICAL RESEARCH LETTERS, VOL. 28, NO. 6, PAGES 1135-1138, MARCH 15, 2001

The electron and proton aurora as seen by IMAGE-FUV and FAST

H. U. Frey,[1] S. B. Mende,[1] C. W. Carlson,[1] J.-C. Gérard,[2] B. Hubert,[2] J. Spann,[3] R. Gladstone,[4] T. J. Immel[1]

Abstract. The Far Ultraviolet Instrument (FUV) on the IMAGE spacecraft observes the aurora in three different channels. One of them (SI12) is sensitive to the signal from precipitating protons, while the other two (WIC and SI13) observe auroral emissions which are not only excited by precipitating electrons, but also by protons. We examine a period when in-situ particle measurements by the FAST spacecraft were available simultaneously with global imaging with FUV. The measured electron and proton energy spectra are used to calculate the auroral brightness along the FAST orbit. The comparison with the FUV/IMAGE observations shows good quantitative agreement and demonstrates that under certain circumstances high proton fluxes may produce significant amounts of auroral FUV emission.

1. Introduction

The main objective of the IMAGE mission is to improve the understanding of magnetospheric processes. One signature of the interaction between the magnetosphere and ionosphere is the creation of aurora. Observations of the global aurora can provide important context information supplementing the direct imaging of the magnetosphere. Previously flown satellites have demonstrated the suitability of far ultra-violet imaging for remote sensing observations of auroral precipitation (see e.g. [*Frank and Craven*, 1988]). The major objective of the Far Ultraviolet Instrument (FUV) on IMAGE is the observation of global changes of the aurora in accordance with large-scale changes in the magnetosphere [*Mende et al.*, 2000]. FUV consists of the Wideband Imaging Camera (WIC), the dual-channel Spectrographic Imager (SI12 and SI13) and the Geocorona Imager (GEO). One feature of FUV is the capability for simultaneous operation in all three wavelength regions. Previously flown imagers had to change filters between exposures which introduced the temporal uncertainty.

[1]SSL, University of California, Berkeley
[2]LPAP, University de Liège, Belgium
[3]MSFC, Huntsville
[4]Southwest Research Institute, San Antonio

Paper number 2000GL012352.
0094-8276/01/2000GL012352$05.00

Generally the auroral oval is not made out of just one luminous structure. Ground based observations usually show many parallel arcs. High-resolution in-situ measurements from satellites resolve these small scales. Space-borne optical instruments have to deal with problems such as the fast motion of the satellite, the large distance to the aurora etc., and therefore only allowed investigation of large structures [*Murphree et al.*, 1994].

Satellite-based optical observations have been combined with in-situ localized measurements of fields and particles (see e.g. [*Johnson et al.*, 1998]). A different approach is the combination of high spatial resolution optical observations from the ground with the localized measurements by satellites. For instance *Frey et al.* [1998] combined ground-based optical observations with measurements from the Freja satellite and demonstrated a good correspondence of the observed brightness with the corresponding particle flux measurements along the track of the satellite. The problem with this approach is that the number of coincident observations is small. The combination of Polar UVI imaging observations with in-situ measurements by DMSP was used to remotely determine the auroral energy characteristics [*Germany et al.*, 1997]. The correspondence was good in the lower latitude part but not as good in the more active poleward part of the aurora. Another study showed that temporal variability of the hemispheric power derived from Polar-UVI images represented a substantial improvement compared to estimates from measurements by the NOAA/TIROS satellites [*Lummerzheim et al.*, 1997]. Quantitative comparisons of energy flux measured by FAST and inferred from remote sensing of the aurora by the Polar UVI indicate good agreement during quiet times. However, poor agreement occurs during disturbed periods, where the inferred energy flux from UVI is generally higher than that measured by FAST [*Chua et al.*, 2000].

This paper shows a detailed quantitative comparison between in-situ FAST measurements and simultaneous FUV observations.

2. Instrumentation and data analysis

The IMAGE satellite describes a highly elliptical orbit of 1000 x 45600 km altitude. FUV observes the aurora during a short period of 5-10 seconds during every 2 minute spin period. WIC has a passband of 140-180 nm with a very small sensitivity below 140 nm. It measures emissions from the N_2 LBH-band, atomic NI lines, and

small contributions from the OI 135.6 nm line. The SI-12 channel is sensitive to the Doppler-shifted Lyman-α emission around 121.8 nm from charge-exchanging precipitating protons. The SI-13 channel has a passband of 5 nm around the 135.6 nm doublet of oxygen OI emission, however, the measured signal is a combination of OI and some bands of the N_2 LBH emission.

Auroral emissions can either be excited by precipitating electrons or protons [*Strickland et al.*, 1993]. Most auroral emissions do not contain information about the identity of the exciting particle, as they originate from oxygen and nitrogen atoms/molecules/ions of the upper atmosphere. Only the emission from hydrogen atoms can be used to derive information about the precipitating particle itself.

The laboratory and star calibrations determined a WIC field of view of 17.2°. For a transformation of the WIC signal into auroral surface brightnesses, the WIC passband and the spectral characteristics of the emission have to be taken into account.

3. Observations

FAST orbit 15226 (June 24, 2000, 0610-0650 UT) was selected for this investigation because FAST measured not only high downgoing electron fluxes, but also a substantial ion flux at the equatorward boundary of the auroral oval.

Figure 1 shows the WIC, SI12 and SI13 images together with the mapped position of FAST. The snapshot time of 06:22:20 UT was selected when FAST had already left the equatorward region with high ion precipitation but was just in the area of bright emission from electron precipitation. The spatial resolution of the in-situ measurements by FAST is much better than the spatial resolution in the FUV images. FAST measures only along the flight path, while FUV observes the whole three-dimensional structure of the aurora. Each pixel contains contributions from emissions away from the FAST track. The spatial scale of any given feature varies with its distance from the true nadir location. This introduces some loss of resolution for features appearing close to the limb. For the instrument settings used during this time period the point-spread-function of WIC had a FWHM of 4.0 pixels in the horizontal direction. For a direct comparison the FAST measurements were mapped down and averaged over a time period corresponding to the size of one FWHM at 100 km altitude, taking into account the change of spatial scale with distance from the limb. The result of this averaged energy flux is given as the full (electrons) and dashed lines (ions) in Figure 2.

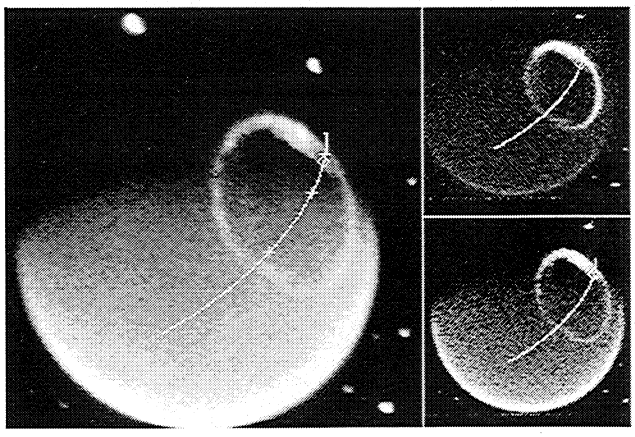

Figure 1. Images taken by WIC (left), SI12 (upper right) and SI13 (lower right) during the FAST orbit 15226 (June 24, 2000, 06:22:20 UT). The footpoint of the FAST track is given by the lines through each image, the position at the snapshot time of the image is shown by a diamond. Local midnight is at the top of the image and FAST first crosses the night part of the auroral oval and then moves to the dayside part. Plus signs mark the location of FAST at 06:20, 06:30, and 06:40, respectively.

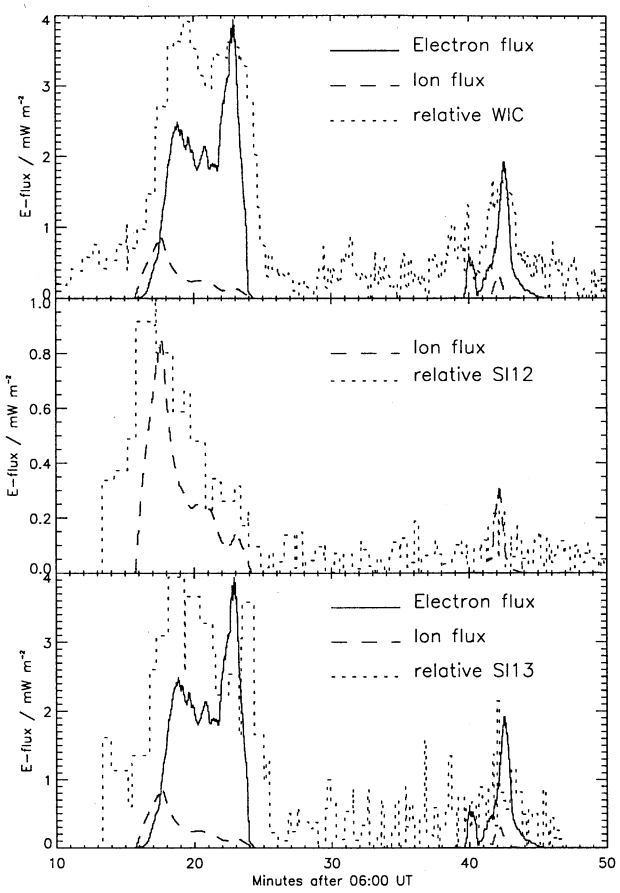

Figure 2. Averaged measured electron (solid line) and ion energy fluxes (dashed line) at orbit 15226 after they were mapped down from the FAST location to 100 km altitude. The relative brightness tracks (dotted lines) along the FAST footpoint during the transit through the FUV images are given for WIC (upper panel), SI12 (middle panel) and SI13 (lowest panel). For each FUV snapshot time a plus-minus one minute part was extracted and the individual tracks are shown according to the time of the FAST in-situ measurements.

FAST moves about 700 km between two FUV snapshots ($\Delta t = 2$ min). Out of each individual FUV image the instrument response was extracted along the track of FAST from the position one minute before to one minute after the snapshot time. This way a continuous brightness track was extracted from 20 individual images. These brightness tracks are shown in Figure 2 after WIC and SI13 have the background from dayglow removed using the method of *Immel et al.*, [2000]. The SI12 image and brightness track show that this channel does not suffer from dayglow background. The bright signal in the dusk pre-midnight part of the SI12 image (right part of image) is furthermore an indicator that this channel is not sensitive to electron induced aurora, because the same region is comparably dim in the WIC and SI13 images.

There is a clear peak of ion precipitation at the equatorward boundary of the auroral oval which coincides well with the peak in the SI12 signal. Further poleward the ion precipitation decreases and overlaps with the electron precipitation which, in contrast to the ions, peaks at the poleward boundary of the oval. The energy flux at the dayside part of the oval is much smaller than on the nightside. From just a visual comparison in the WIC channel it is clear that the two peaks in the WIC signal do not correspond to a similar structure in the electron energy flux.

The electron and ion spectra in the loss cone from the FAST measurements were used as input for a full-code simulation of the production of auroral FUV emissions [*Hubert et al., 2000*]. The methodology adopted to calculate the excitation rates rests on the combination of two transport models which respectively describe the interaction of an electron and a proton beam with the atmosphere and, which together account for collisional energy degradation, the generation of a neutral H beam following collisions with protons and the production of secondary electrons [*Solomon et al.*, 1988; *Solomon*, 2000; *Gerard et al.*, 2000]. The resulting volume excitation rates for the N_2 LBH bands and the NI 149.3 nm emission are calculated including all collisional excitation processes. The emerging intensities are obtained by integration along the line of sight. The result of this simulation was then convolved with the WIC passband to calculate the expected signal in the WIC image. The simulations indicate that the LBH and 135.6 nm emissions may contain significant contributions from proton excitation. The intensity of the LBH emission is mostly determined by the precipitating energy flux. However, high-energy electrons may penetrate to lower altitudes where the O_2 Schumann-Runge absorption continuum significantly reduces the observed LBH intensity. The full simulation code includes this absorption assuming moderately disturbed conditions during solar maximum, but quantitative analysis of auroral energetics using global observations will always suffer from the unknown peak energy of precipitating electrons unless higher spectral resolution images are available.

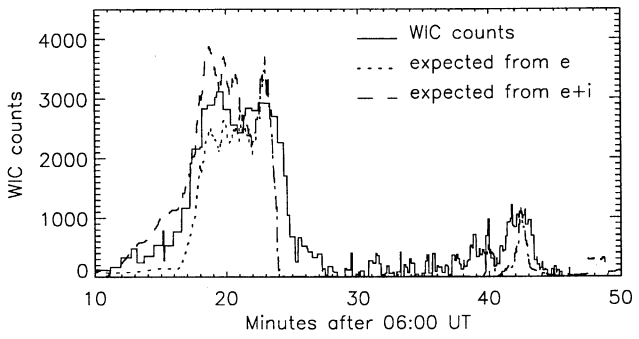

Figure 3. Comparison of the expected WIC signal from simulations using the FAST measurements during orbit 15226 and the real WIC signal. The solid line gives the AD units measured by WIC along the FAST footpoints. The dotted line is the expected WIC signal from in-situ measurements of the precipitating electron flux. The dashed line is the expected WIC signal for the combined auroral emissions from electron and ion precipitation.

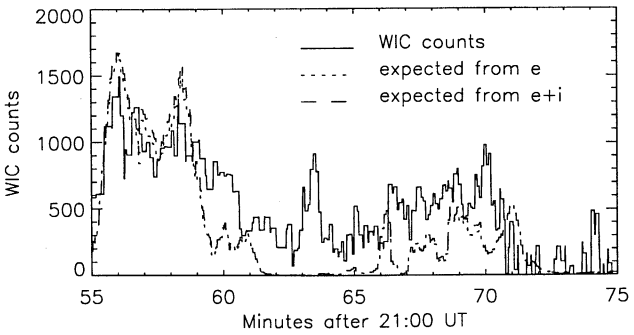

Figure 4. Same as Figure 3 for orbit 15244.

Figure 3 shows the result of two comparisons. Taking the expected brightness from simulations with the electron precipitation only, we obtain an overestimation at the poleward part of the nightside auroral oval. At the equatorward part of the nightside auroral oval however, the expected signal from electron precipitation is only about 70-80 % of the measured WIC signal. If the simulation also includes the ion precipitation, then a much better overall agreement between the expected and obtained WIC signal is reached. The expected signal is now everywhere overestimated by 30 %, a good agreement considering the different spatial and time resolution of the FAST and IMAGE measurements and the uncertainties in instrumental calibrations.

Another FAST orbit with simultaneous FUV observations was 15244 (June 25, 2000, around 2200 UT). The mean electron energy flux was only half the flux from orbit 15226, but the ion flux was almost 10 times smaller (not shown). The comparison between the expected and obtained WIC signal is given in Figure 4. As expected the electron flux accounts for almost all WIC signal and the ion flux just adds a small additional sig-

nal. Again the expected signal is about 30 % larger at the peaks than the obtained signal. The peak in the WIC signal at 22:04 comes from a transient structure. The FAST spectrum could not be modeled as well as in other cases and therefore the result was discarded. The overestimation of the signal at the midnight part of the oval is expected because the simulation assumes a horizontally homogeneous precipitation. The integration along the line of sight will then produce overestimated signals at the local peaks of precipitation. At the dayside aurora the look direction is close to the nadir and here we obtain a good agreement or an underestimate, respectively.

4. Conclusions

The FUV instrument on IMAGE observes the aurora in three different channels. One of those channels is purely sensitive to precipitating protons (SI12). The other two channels observe portions of the auroral spectrum which are not only excited by electron precipitation, but also by proton precipitation.

Simultaneous observations combining data from two orbits of FAST in-situ particles measurements with IMAGE FUV global remote sensing give good agreement between predicted and observed emission rates. This comparison also shows that under certain circumstances the precipitating protons may produce significant amounts of auroral emissions usually associated with electron precipitation. If this emission is ignored or cannot be measured, then the result of calculations based on the assumption of pure electron precipitation will overestimate the electron flux.

For the case of IMAGE FUV the presence of the SI12 channel allows for the determination of the proton flux and a corresponding correction to the electron flux estimated from the WIC and SI13 channels. A quantitative comparison will be the topic of a forthcoming paper.

Acknowledgments. The FUV team appreciates the support by the IMAGE SMOC. J.C.G. is supported by the Belgian National Fund for Scientific Research (FNRS). This work was partly funded by the PRODEX program of the European Space Agency (ESA) and the Belgian Fund for Collective Fundamental Research (Grant FRFC 97-2.4569.97).

References

Chua, D., G. Parks, M. Brittnacher, W. Peria, G. Germany, J. Spann, C. W. Carlson, Energy characteristics of auroral electron precipitation: A comparison of substorms and pressure pulse related auroral activity, *J. Geophys. Res.*, in press, 2000.

Frank, L. A. and J. D. Craven, Imaging results from Dynamics Explorer 1, *Rev. Geophys., 2,* 249, 1988.

Frey, H. U. et al., Freja and ground-based analysis of inverted-V events, *J. Geophys. Res., 103,* 4303, 1998.

Germany, G. A. et al., Remote determination of auroral energy characteristics during substorm activity, *Geophys. Res. Lett., 24,* 995, 1997.

Gérard, J.-C., B. Hubert, H., D. V. Bisikalo and V. I. Shematovich, A model of the Lyman-α line profile in the proton aurora, *J. Geophys. Res., 105,* 15795, 2000.

Hubert, B., J.-C. Gérard, D. V. Bisikalo and V. I. Shematovich, The role of proton precipitation in the excitation of auroral FUV emissions, submitted, 2000.

Immel, T. J., J. D. Craven and A. C. Nicholas, The DE-1 auroral imager's response to the FUV dayglow for thermosperic studies, *J. Atmos. Solar-Terr. Phys., 62,* 47, 2000.

Johnson, M. L., J. S. Murphree, G. T. Marklund, and T. Karlson, Progress on relating optical auroral forms and electric field patterns, *J. Geophys. Res., 103,* 4271, 1998.

Lummerzheim, D. et al., High time resolution study of the hemispheric power carried by energetic electrons into the ionosphere during the May 19/20, 1996 auroral activity, *Geophys. Res. Lett., 24,* 987, 1997.

Mende, S. B. et al., Far ultraviolet imaging from the IMAGE spacecraft, *Space Sci. Rev., 91,* 287, 2000.

Murphree, J. S., M. L. Johnson, L. L. Cogger, and D. J. Hearn, Freja UV imager observations of spatially periodic auroral distortions, *Geophys. Res. Lett., 21,* 1887, 1994.

Solomon, S. C., P. B. Hays and V. Abreu, The auroral 6300 A emission: observation and modelling, *J. Geophys. Res., 93,* 9867, 1988.

Solomon, S. C., Auroral particle transport using Monte Carlo hybrid methods, *J. Geophys. Res., 105,* 2000.

Strickland, D. J., R. E. Daniell, J. R. Jasperse, and B. Basu, Transport-theoretic model for the electron-proton-hydrogen atom aurora, 2. Model results, *J. Geophys. Res., 98,* 21533, 1993.

C. W. Carlson, H. U. Frey, S. B. Mende, T. J. Immel, Space Sciences Laboratory, University of California, Berkeley, CA 94720-7450 (e-mail: hfrey@ssl.berkeley.edu)

J. C. Gérard, B. Hubert, LPAP, Université de Liège, B-4000 Liège, Belgium (e-mail: gerard@astro.ulg.ac.be)

J. Spann, George C. Marshall Spaceflight Center, Huntsville, AL 35812 (e-mail: jspann@hq.nasa.gov)

R. Gladstone, Southwest research Institute, San Antonio, TX 78228 (e-mail: randy@whistler.space.swri.edu)

(Received September 19, 2000; accepted October 27, 2000.)